Quasi-adiabaticity in bifurcated current sheets.

Dominique C. Delcourt, H. V. Malova, L. M. Zelenyi

Quasi-adiabaticity in bifurcated current sheets

D. C. Delcourt,[1] H. V. Malova,[2] and L. M. Zelenyi[3]

Received 12 December 2005; revised 10 January 2006; accepted 3 February 2006; published 21 March 2006.

[1] We examine the non-linear dynamics of charged particles in "bifurcated" (double-humped) current sheets. We show that, when the adiabaticity parameter κ is of the order unity, particles experience a negligible change of magnetic moment. Such a behavior contrasts with the prominent magnetic moment scattering that is achieved in single-humped current sheets at such κ values. It resembles the quasi-adiabatic (Speiser-type) behaviors that is obtained at $\kappa \ll 1$ as a result of resonance between the fast oscillation about the midplane and the slow gyromotion near this plane. We demonstrate that beams of $\kappa \approx 1$ particles may form downstream of bifurcated current sheets, which propagate along the magnetic field lines up to high latitudes. Quasi-adiabaticity and associated beam formation thus occur at significantly larger κ values in double-humped current sheets than in single-humped ones, or equivalently for lower particle energy and/or weaker field reversal. **Citation:** Delcourt, D. C., H. V. Malova, and L. M. Zelenyi (2006), Quasi-adiabaticity in bifurcated current sheets, *Geophys. Res. Lett.*, *33*, L06106, doi:10.1029/2005GL025463.

1. Introduction

[2] Thin current sheets (TCS) are well known phenomena in the Earth's magnetosphere [e.g., *Mitchell et al.*, 1990; *Pulkkinen et al.*, 1993, 1994] but it is only recently that in-situ measurements provided evidences of a possible "bifurcated" or double-humped structure for such TCS [e.g., *Hoshino et al.*, 1996; *Runov et al.*, 2003, 2006; *Sergeev et al.*, 2003]. This structure is at variance with the single-humped one that is commonly postulated in the magnetotail [e.g., *Harris*, 1962]. Different mechanisms have been proposed to explain these bifurcations such as a large electron Hall current on both sides of the current sheet midplane [e.g., *Hoshino et al.*, 1998], a current reduction at the sheet center due to inclusion of quasi-trapped ions [e.g., *Zelenyi et al.*, 2002] or diffusion due to electromagnetic fluctuations [e.g., *Greco et al.*, 2002]. As far as the charged particle dynamics is concerned, it was shown in *Delcourt et al.* [2004] that, in both single- and double-humped current sheets, scattering of the magnetic moment may be viewed as the result of perturbation of the particle gyromotion by an impulsive centrifugal force. However, the net change of magnetic moment varies in these current sheets because of two successive perturbations in one case as compared to a single one in the other case. In the present study, we show that magnetic moment variations may considerable weaken in double-humped current sheets when the Larmor radius is comparable to the field variation length scale, a dynamical feature that is referred to as quasi-adiabaticity. We demonstrate that this leads to the formation of accelerated ion beams along the magnetic field lines, which contrasts with the chaotic motion that is obtained in single-humped current sheets.

2. Magnetic Moment Scattering in Double-Humped Current Sheets

[3] To perform a comparative analysis of the change of magnetic moment (hereinafter denoted by $\mu = mV^2\sin^2\alpha/2B$ where V is the particle speed, m, its mass, and α, the pitch angle) in single- and double-humped current sheets, we consider on one hand the parabolic field defined as: $B_X = B_o Z/L$, $B_Z = B_n$, and on the other hand the double-humped model used in *Delcourt et al.* [2004] (hereinafter referred to as paper 1), viz.,

$$B_X = B_0\left[10\frac{Z^3}{L^3} - 15\frac{Z^4}{Z^4} + 6\frac{Z^5}{L^5}\right] \quad (1)$$

$$B_Z = B_n \quad (2)$$

In these equations, L is the current sheet half-thickness, B_n, the small component of the magnetic field normal to the midplane, and B_o, the asymptotic B_X component in the lobe. With these simple models, our intent is to investigate μ-scattering when the particles interact with the field reversal, or equivalently in the $|Z| \leq L$ domain. In this domain, as pointed out by *Büchner and Zelenyi* [1989], parabolic field and Harris sheet are fairly similar and the results in both cases nearly are identical. At large Z heights ($Z \gg L$), particles are trapped in the former model while they escape to infinity in the latter one [see, e.g., *Chen*, 1992], but this is not of relevance for the present study. As for the double-humped case, the model used here differs from recent attempts to describe bifurcated current sheets [e.g., *Schindler and Birn*, 2002; *Sitnov et al.*, 2003]. However, it provides a qualitative description of a bifurcated sheet with current density maxima on either side of the $Z = 0$ plane near $B = 0.5\ B_o$ (see paper 1, Figure 1), which is consistent with in-situ measurements [e.g., *Runov et al.*, 2003, 2006; *Sergeev et al.*, 2003].

[4] The magnetic field lines obtained in these two models are shown in Figure 1. It can be seen in this figure that the maximum field line curvature is obtained at equator in the parabolic field (dotted lines) and off-equator in the double-humped one (solid lines). In the parabolic case, the adiabaticity parameter κ introduced by *Büchner and Zelenyi*

[1]Centre d'étude des Environnements Terrestre et Planétaires, Centre National de la Recherche Scientifique, Institut Pierre-Simon Laplace, Saint-Maur des Fossés, France.
[2]Nuclear Physics Institute, Moscow State University, Moscow, Russia.
[3]Space Research Institute, Russian Academy of Sciences, Moscow, Russia.

0094-8276/06/2005GL025463

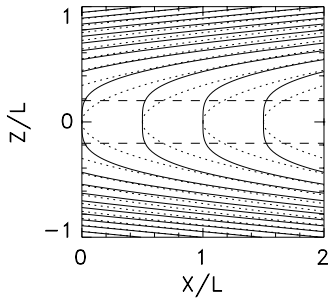

Figure 1. Magnetic field lines in the single- (dotted lines) and double-humped (solid lines) models considered in this study. The horizontal dashed line shows the Z height at which κ_{eff} is calculated in the double-humped case.

[1989] (defined as the square root of the minimum curvature radius-to-maximum Larmor radius ratio, viz., $\kappa = [R_{C\ min}/\rho_{L\ max}]^{1/2}$) can be evaluated at $Z = 0$ which is also the locus of minimum magnetic field magnitude. In contrast, in the double-humped case, the maximum field line curvature and the minimum B magnitude do not coincide so that an effective parameter κ_{eff} was introduced by paper 1, defined as the minimum κ value encountered along the field line. The horizontal dashed line in Figure 1 shows the Z height at which κ_{eff} is calculated.

[5] In order to explore the particle diffusion toward small and large pitch angles upon interaction with the field reversal, we consider the case of a beam incident upon the midplane, as expected for instance from pitch angle folding for particles traveling from large to small B regions. In a like manner to *Sergeev et al.* [1983], we assume the inflowing distribution to be empty inside the loss cone and isotropic for pitch angles between 3° and 10° (note that these pitch angles are evaluated at equator in the adiabatic limit, i.e., assuming μ-conservation). To reconstruct the flux variations due to nonadiabatic transport in the field reversal, we performed trajectory computations in both models, using the following parameter values: $B_o = 10$ nT, $B_n = 1$ nT, and $L = 1$. Distinct κ values between 3 and 1 were also considered. As emphasized in previous studies [e.g., *Sergeev et al.*, 1983; *Büchner and Zelenyi*, 1989], it should be kept in mind here that κ controls the charged particle dynamics so that, for given κ, the particle behavior is not affected by changing the above values of B_o, B_n, or L although the particle energy will be different in each case.

[6] The results of these calculations are shown in Figure 2 that presents the directional differential flux versus pitch angle at equator. Looking first at the profiles obtained in the parabolic case (dotted lines), it can be seen that, as κ decreases from 3 to 1, μ-scattering is more and more pronounced. As discussed by *Sergeev et al.* [1983], this scattering is characterized by significant filling of the loss cone at $\kappa \approx 2$ and diffusion toward large pitch angles at smaller κ. A similar behavior is obtained if a Harris sheet is considered in place of the present parabolic field. On the other hand, the solid lines in Figure 2 display a different evolution in the case of a double-humped model. Here, substantial filling of the loss cone is obtained at $\kappa = 2.7$ and $\kappa = 2.3$, whereas minor pitch angle change can be seen at $\kappa = 2.5$. As κ further decreases toward 1, diffusion toward large pitch angles is noticeable. However, in contrast to the parabolic case, this diffusion maximizes near $\kappa \approx 1.7$ and considerably weakens for $\kappa \approx 1$. At this latter κ value, it is apparent that a number of ions experience weak μ variations and substantial loss cone filling is obtained.

[7] It was shown by paper 1 that, in a double-humped current sheet, μ-scattering may be viewed as the result of two successive perturbations of the particle gyromotion by an impulsive centrifugal force. Although each of these perturbations lead to a characteristic three-branch pattern of μ variations (with large increase at small pitch angles, negligible change at large pitch angles, and possible damping in between), the net μ change after crossing of the field reversal does not exhibit such a clear structure. The evolution portrayed in Figure 2 directly follows from these combined centrifugal perturbations. Still, systematic computations performed with different sets of B_o, B_n, and L values reveal that the results in Figure 2 are robust, with significant μ attenuation for κ immediately below 3 ($\kappa \approx 2.5$) and for $\kappa \approx 1$.

[8] For particles traveling through a field reversal, $\kappa \approx 3$ delineates the transition between adiabatic and nonadiabatic behaviors [e.g., *Sergeev et al.*, 1983; *Büchner and Zelenyi*, 1989]. As illustrated in Figure 2, at $\kappa < 3$, μ-scattering is responsible for particle injection into the loss cone, a behavior that may be used to derive information on the magnetotail field line elongation as featured, for example, in the Isotropic Boundary Algorithm of *Sergeev et al.* [1993]. As for the $\kappa \approx 1$ limit, it is commonly regarded as a regime of enhanced pitch angle diffusion [e.g., *Büchner and Zelenyi*, 1989]. However, what Figure 2 demonstrates is that this latter view applies to single-humped current sheets but not to double-humped ones. In this case, $\kappa \approx 1$ particles experience a weak μ change, which is of importance for the

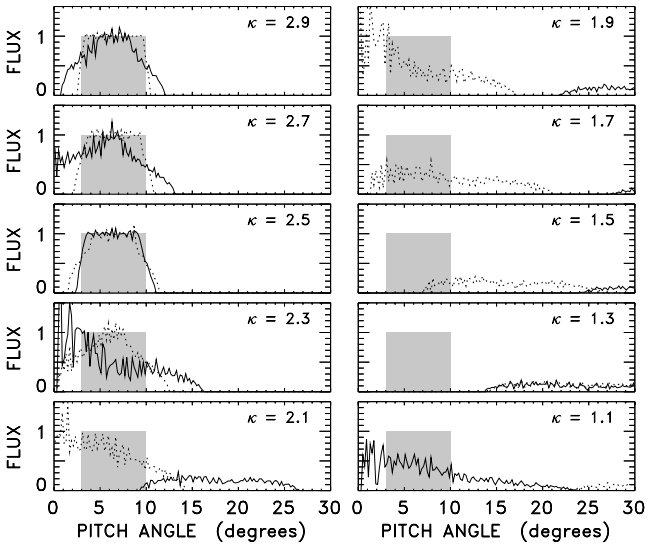

Figure 2. Directional differential flux (normalized to 1) as a function of pitch angle for distinct κ values. Dotted and solid lines correspond to parabolic case and double-humped case, respectively. The initial distribution (shaded area) is assumed to be isotropic between 3° and 10°.

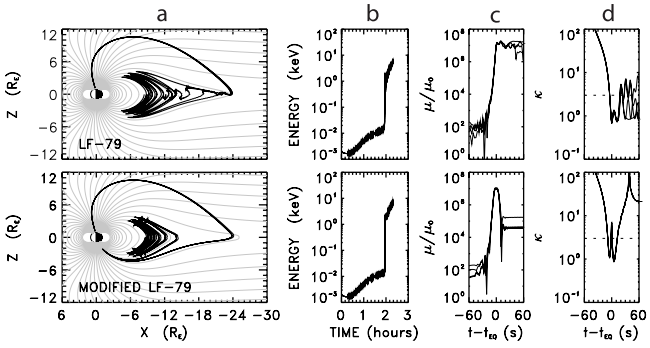

Figure 3. Results of the simulations in the (top) original and (bottom) modified LF-79: (a) Model H^+ trajectory projection in the noon-midnight plane, (b) energy versus time, (c) magnetic moment (normalized to initial value) and (d) instantaneous κ versus time (measured from that of the first equatorial crossing). The test H^+ are launched with 2 eV energy and four distinct gyration phases from the noon region.

magnetotail dynamics as will be seen in the following section.

3. Ion Beamlets at $\kappa \approx 1$

[9] In an early study, *Chen and Palmadesso* [1986] put forward that, for some specific κ values (< 1), particles preferentially execute Speiser-type orbits [*Speiser*, 1965] whereas, for other values of κ (< 1), most of the particles experience prominent μ-scattering and are temporarily trapped inside the current sheet. This feature was interpreted as the result of a resonance between the fast meandering motion about the midplane and the slow gyromotion about the small B_n. The following empirical relationship was derived to characterize the ith resonance:

$$\kappa_i = \frac{0.8}{i + 0.6} \tag{3}$$

According to (3), the first resonance occurs at $\kappa \approx 0.5$, the second one at $\kappa \approx 0.31$, the third one at $\kappa \approx 0.22$ and so forth. These resonances are analogous to the quasi-adiabatic regime put forward by *Büchner and Zelenyi* [1989] at $\kappa \ll 1$. In this regime, particles experience a negligible change of the invariant $I_Z = \int \dot{z}\, dz$ and behave in a nearly adiabatic manner. Unlike trapped or quasi-trapped particles, quasi-adiabatic (resonant) particles experience a large energization upon a single interaction with the current sheet and subsequently escape toward high latitudes, leading to multiple ion beams or "beamlets" as commonly observed in the outer plasma sheet [e.g., *Ashour-Abdalla et al.*, 1996; *Sauvaud and Kovrazhkin*, 2004].

[10] The results presented above suggest that, in the event that a bifurcated current sheet forms in the magnetotail, such a quasi-adiabatic regime may be obtained at $\kappa \approx 1$. This is of importance, for example, for low-energy ions that originate from the topside ionosphere, which often exhibit $\kappa \approx 1$ upon interaction with the tail current sheet. This is illustrated in Figure 3 that shows the results of trajectory computations for H^+ originating from the dayside cusp. Two distinct current sheet structures have been considered in this figure, with single-humped case in the top panels of Figure 3 and double-humped case in the bottom ones. These distinct field configurations were obtained using the *Luhmann and Friesen* [1979] model (LF-79), considering either the original version that consists of a Harris-type current sheet superposed onto the Earth's dipole or a modified one where the superposed current sheet is that given in (1)–(2).

[11] Regardless of the magnetic field model, it can be seen in Figure 3 that the test H^+ are transported from the dayside cusp into the nightside sector over the polar cap under the effect of the large scale convection electric field. In the magnetospheric lobe, the ions are centrifugally accelerated up to ~100 eV (Figure 3b) and they subsequently intercept the equatorial plane near $X = -24$ R_E. At this point, although the test H^+ have $\kappa \approx 1$ in both cases (Figure 3d), it is apparent that their interaction with the field reversal radically differs depending upon the current sheet structure, viz. In the original LF-79 (Figure 3 (top)), ions are subjected to large μ enhancements regardless of gyration phase. This leads to mirroring at high altitudes immediately followed by repeated interactions with the current sheet. In contrast, in the modified LF-79 (Figure 3 (bottom)), the large μ enhancement experienced by the ions before crossing of the midplane is immediately followed by a μ decrease, consistently with the interpretation framework developed by paper 1 that invokes two successive centrifugal perturbations. Because the net μ change is here much weaker, the cusp originating H^+ subsequently travel toward high latitudes in the opposite hemisphere and ultimately mirror at low altitudes with energies of several keVs due to acceleration upon current sheet crossing.

[12] As mentioned above, though it occurs at $\kappa \approx 1$, the ion behavior portrayed in Figure 3 (bottom) with successive μ increase and decrease is reminiscent of the quasi-adiabatic one of *Büchner and Zelenyi* [1989] with successive I_Z jumps that nearly cancel each other. The adiabatic-like character of the H^+ trajectories in Figure 3 (bottom) can be better appreciated by comparison with Figure 4 that shows the trajectories obtained for the same ions but using a guiding center treatment. Because μ conservation is here imposed throughout transport, the test H^+ travel back to low altitudes after a single crossing of the current sheet and ultimately precipitate into the opposite hemisphere. This behavior clearly resembles that portrayed in Figure 3 (bottom).

[13] To provide a more comprehensive view of this effect, we performed systematic trajectory computations in both original and modified LF-79, considering test H^+ with different energies, pitch angles and gyration phases. These H^+ were launched from a point source in the midnight meridian plane. The results of these computations are summarized in Figure 5 that shows mirror point altitudes as a function of κ. A striking feature in this figure is the

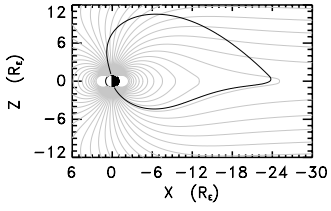

Figure 4. Identical to Figure 3 (bottom) but using a guiding center treatment.

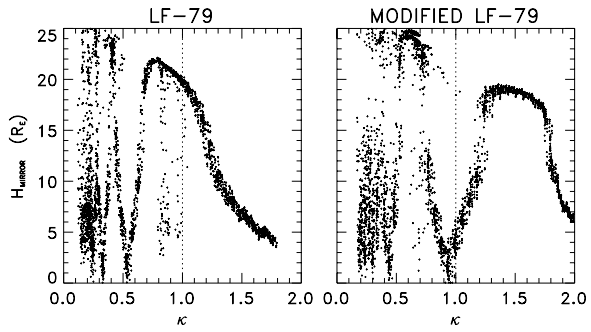

Figure 5. Mirror point altitude as a function of κ in the (left) original LF-79 and (right) modified LF-79. The H^+ are launched with different energies (from 10 eV up to 10 keV), pitch angles (from 150° up to 180°) and gyration phases (from 0° to 360°) from a point source located at $X = -20\ R_E$ and $Z = 2\ R_E$.

low-altitude (possibly down to ionospheric height) mirror points achieved for $\kappa \approx 1$ in the modified LF-79 (right), which contrasts with the high-altitude ones obtained for this very κ value in the original LF-79 (left). A modulation of the mirror point altitude is also apparent for $\kappa \leq 0.5$, due to resonant and non-resonant behaviors. In this latter κ range, qualitatively similar patterns are obtained in Figure 5, the low-altitude mirror points occurring approximately at the κ values given by (3). Figure 5 thus clearly displays that, in the case of bifurcated current sheets, accelerated ions that travel down to low altitudes in the outer plasma sheet may not necessarily follow from Speiser-type orbits at $\kappa \ll 1$ but possibly from quasi-adiabatic behavior at $\kappa \approx 1$.

4. Conclusion

[14] The numerical simulations performed demonstrate that the $\kappa \approx 1$ dynamical regime significantly differs in single- and double-humped current sheets. Whereas particles are subjected to prominent μ scattering in the former case, they exhibit negligible μ change in the latter case, a behavior which resembles the quasi-adiabatic one that occurs at $\kappa \ll 1$. In the magnetotail, this can lead to the formation of accelerated ion beams downstream of bifurcated current sheets, which subsequently propagate along the magnetic field lines in the outer plasma sheet down to low altitudes. With $\kappa \approx 1$, these beams are obtained at lower energies and/or for weaker field reversal than in the case of single-humped current sheets.

[15] **Acknowledgment.** The work by H. V. Malova and L. M. Zelenyi was partially supported by RFBR grants 05-02-17003, 04-02-17371, 05-05-64993, GFEN 04-02-39021, INTAS 03-51-3738 and Scientific Schools grant HIII-1739.2003.2.

References

Ashour-Abdalla, M., L. A. Frank, W. R. Paterson, V. Peroomian, and L. M. Zelenyi (1996), Proton velocity distributions in the magnetotail: Theory and observations, *J. Geophys. Res.*, *101*, 2587.

Büchner, J., and L. M. Zelenyi (1989), Regular and chaotic charged particle motion in magnetotaillike field reversals: 1. Basic theory of trapped motion, *J. Geophys. Res.*, *94*, 11,821.

Chen, J. (1992), Nonlinear dynamics of charged particles in the magnetotail, *J. Geophys. Res.*, *97*, 15,011.

Chen, J., and P. J. Palmadesso (1986), Chaos and nonlinear dynamics of single-particle orbits in magnetotaillike magnetic field, *J. Geophys. Res.*, *91*, 1499.

Delcourt, D. C., H. V. Malova, and L. M. Zelenyi (2004), Dynamics of charged particles in bifurcated current sheets: The $\kappa \approx 1$ regime, *J. Geophys. Res.*, *109*, A01222, doi:10.1029/2003JA010167.

Greco, A., A. L. Taktakishvili, G. Zimbardo, P. Veltri, and L. M. Zelenyi (2002), Ion dynamics in the near-Earth magnetotail: Magnetic turbulence versus normal component of the average magnetic field, *J. Geophys. Res.*, *107*(A10), 1267, doi:10.1029/2002JA009270.

Harris, E. G. (1962), On a plasma sheath separating regions of oppositely directed magnetic fields, *Nuovo Cimento*, *23*, 115.

Hoshino, M., A. Nishida, T. Mukai, Y. Saito, T. Yamamoto, and S. Kokubun (1996), Structure of plasma sheet in magnetotail: Double-peaked electric current sheet, *J. Geophys. Res.*, *101*, 24,775.

Hoshino, M., T. Mukai, T. Yamamoto, and S. Kokubun (1998), Ion dynamics in magnetic reconnection: Comparison between numerical simulation and Geotail observations, *J. Geophys. Res.*, *103*, 4509.

Luhmann, J. G., and L. M. Friesen (1979), A simple model of the magnetosphere, *J. Geophys. Res.*, *84*, 4405.

Mitchell, D. G., D. J. Williams, C. Y. Huang, L. A. Frank, and C. T. Russell (1990), Current carriers in the near-Earth cross-tail current sheet during substorm growth phase, *Geophys. Res. Lett.*, *17*, 583.

Pulkkinen, T. I., D. N. Baker, C. J. Owen, J. T. Gosling, and N. Murphy (1993), Thin current sheets in the deep geomagnetotail, *Geophys. Res. Lett.*, *20*, 2427.

Pulkkinen, T. I., D. N. Baker, D. G. Mitchell, R. L. McPherron, C. Y. Huang, and L. A. Frank (1994), Thin current sheets in the magnetotail during substorms: CDAW 6 revisited, *J. Geophys. Res.*, *99*, 5793.

Runov, A., R. Nakamura, W. Baumjohann, T. L. Zhang, M. Volwerk, H.-U. Eichelberger, and A. Balogh (2003), Cluster observation of a bifurcated current sheet, *Geophys. Res. Lett.*, *30*(2), 1036, doi:10.1029/2002GL016136.

Runov, A., et al. (2006), Local structure of the magnetotail current sheet: 2001 Cluster observations, *Ann. Geophys.*, *24*, in press.

Sauvaud, J.-A., and R. A. Kovrazhkin (2004), Two types of energy-dispersed ion structures at the plasma sheet boundary, *J. Geophys. Res.*, *109*, A12213, doi:10.1029/2003JA010333.

Schindler, K., and J. Birn (2002), Models of two-dimensional embedded thin current sheets from Vlasov theory, *J. Geophys. Res.*, *107*(A8), 1193, doi:10.1029/2001JA000304.

Sergeev, V. A., et al. (1983), Pitch-angle scattering of energetic protons in the magnetotail current sheet as the dominant source of their isotropic precipitation into the nightside ionosphere, *Planet. Space. Sci.*, *31*, 1147.

Sergeev, V. A., M. Malkov, and K. Mursula (1993), Testing the isotropic boundary algorithm method to evaluate the magnetic field configuration in the tail, *J. Geophys. Res.*, *98*, 7609.

Sergeev, V., et al. (2003), Current sheet flapping motion and structure observed by Cluster, *Geophys. Res. Lett.*, *30*(6), 1327, doi:10.1029/2002GL016500.

Sitnov, M. I., P. N. Guzdar, and M. Swisdak (2003), A model of the bifurcated current sheet, *Geophys. Res. Lett.*, *30*(13), 1712, doi:10.1029/2003GL017218.

Speiser, T. W. (1965), Particle trajectory in model current sheets: 1. Analytical solutions, *J. Geophys. Res.*, *70*, 4219.

Zelenyi, L. M., D. C. Delcourt, H. V. Malova, and A. S. Sharma (2002), "Aging" of the magnetotail thin current sheets, *Geophys. Res. Lett.*, *29*(12), 1608, doi:10.1029/2001GL013789.

D. C. Delcourt, CETP-CNRS-IPSL, F-94107 Saint-Maur des Fossés, France. (dominique.delcourt@cetp.ipsl.fr)

H. V. Malova, Nuclear Physics Institute, Moscow State University, Moscow 119899, Russia.

L. M. Zelenyi, Space Research Institute, Russian Academy of Sciences, Moscow 117810, Russia.